

Identifications of Auger spectra from 2-MeV foil-excited carbon ions

D. Schneider

Hahn-Meitner-Institut für Kernforschung Berlin GmbH, Glienicke Strasse 100, 1 Berlin 39, West Germany

R. Bruch

Institut für Atom- und Festkörperforschung A, Freie Universität Berlin, Boltzmannstrasse 20, 1 Berlin 33, West Germany

W. H. E. Schwarz and T. C. Chang

Lehrstuhl für Theoretische Chemie, Universität Bonn, Wegelerstrasse 12, 53 Bonn, West Germany

C. F. Moore

Department of Physics, University of Texas at Austin, Austin, Texas 78712

(Received 16 August 1976)

We have measured high-resolution electron decay-in-flight spectra of highly excited carbon ions, produced by 2-MeV C^+ beams emerging from carbon foils. An almost complete identification for the resolved spectral lines is suggested for the prompt and time-delayed electron emission spectra. To assign the observed structures excitation energies for various core-excited states have been calculated using the generalized Brillouin theorem-multiconfiguration method of Schwarz and Chang. Experimental term energies for Coulomb and metastable autoionizing states in two-, three-, and four-electron carbon ions are tabulated and compared to calculated transition energies. Because of line blending most of the experimentally deduced term energies are uncertain to $\pm 0.4\%$. Some spectral features in the high-energy portion of the prompt spectrum can be attributed to decays of doubly excited He-like carbon ions.

I. INTRODUCTION

High-resolution measurements of Auger-electron production in energetic heavy-ion-atom collisions for spectroscopic studies have become a subject of increasing interest. Measurements of K Auger-electron emission from neon target gas after bombardment with highly stripped oxygen and chlorine projectile ions at several MeV have been reported recently.^{1,2} It has been shown that the complexity of the Auger spectra can be reduced by increasing the charge state in conjunction with higher mass of the bombarding particles. This offers the possibility for spectroscopic studies as well as the study of specific excitation and deexcitation mechanisms in highly stripped ions with few electrons. On the other hand, Auger decays from few-electron systems may be studied using the beam-foil method.^{3,4} Beam-foil excitation allows the production of highly stripped ionic states, with the mean ionic charge controllable to some degree. Furthermore, both prompt electron spectra from Coulomb autoionizing states and delayed spectra from metastable autoionizing states can be observed in the same experiment. Because of specific selection rules, the delayed spectra are less complicated than those with the foil in view of the electron spectrometer.

Time-delayed beam-foil Auger-electron emission spectra have been reported for oxygen and fluorine by Donnally *et al.*⁵ and Sellin *et al.*,⁶ for

chlorine and argon by Sellin *et al.*⁷ and Pegg *et al.*,⁸ and for aluminum and silicon by Haselton *et al.*⁹ The emitted electrons result from the decay-in-flight of autoionizing projectile states associated with various charge states present in the foil excited beam. Theoretical predictions for three- to five-electron ions in oxygen and fluorine have been made by Junker and Bardsley.¹⁰ Previous measurements discussed in articles by Pegg *et al.*¹¹ and Sellin¹² have dealt primarily with the study of metastable autoionizing states. The electron decay-in-flight of highly excited beam ions has been measured as a function of distance downstream from an exciter foil, and lifetimes of Li-like $(1s2s2p)^4P_{5/2}^o$ states have been determined. In the course of these experiments attempts have also been made to measure the prompt decaying Coulomb autoionizing states by directly viewing at the back of the carbon foil. These spectra (taken at "zero distance" with the target in direct view) have suffered from background contributions and substantial line broadening, and are essentially unresolved due to many overlapping autoionization features. Consequently, no prompt beam Auger lines were resolved (except the lowest ones), and no detailed line identifications were given.

Johnson *et al.*^{13,14} and Schneider *et al.*¹⁵ reported the first high-resolution measurements of Auger-electron decay of oxygen and carbon ions at MeV energies, excited by collisions with noble

gases and thin carbon foils. A comparison of the prompt electron spectra, produced at 2 and 3 MeV impact energies in the gaseous and solid media showed remarkable similarities in the line structures, intensities, and widths. This points out the possibility for using foil excitation for spectroscopic studies on electron decay-in-flight spectra from sufficiently fast highly stripped projectile ions. No complete spectroscopic assignment of the prompt and delayed electron emission spectra was reported,^{14,15} however, because of a lack of sufficient transition-energy calculations.

In this study we will present for the first time an almost complete interpretation of prompt and time delayed autoionizing transitions in two- to four-electron carbon ions. In order to make assignments in the observed spectra, we performed *ab initio* calculations of term energies in carbon within a few tenths of an eV accuracy. Such core-excited carbon states are of considerable interest since they allow one to study electron correlation effects in few-electron ionic systems. In addition, we found evidence for the decay of metastable autoionizing quartet states in CIV and quintet states in CIII which can only undergo transitions to the adjacent continuum via relativistic interactions (e.g., spin-orbit, spin-other-orbit, and spin-spin coupling) and via admixtures of prompt decaying states (e.g., second-order processes).

II. EXPERIMENTAL

The 2-MeV carbon beam was produced by the University of Texas at Austin model EN tandem Van de Graaff accelerator. Thin carbon foils nominally $\sim 5 \mu\text{g}/\text{cm}^2$ thick were used to excite the carbon beams. In the experimental setup the foil could be moved from "zero distance" (i.e., within the analyzer viewing region) to about 12 cm upstream. This allowed for the study of delayed electron emission as a function of distance downstream from the exciter foil. Electrons ejected from foil excited carbon beams were energy-selected using a 36-cm double-focusing electrostatic analyzer (McPhearson ESCA 36). The analyzer and the automated data-acquisition system have been described in detail previously.^{13,33}

The intrinsic resolution $\Delta E_A/E_A$ of the electron spectrometer is 0.02% (FWHM), where E_A is the electron energy and ΔE_A is the width of the analyzer transmission function. Energy and efficiency calibration of the spectrometer were accomplished by comparison with electron-induced high-resolution Ne K Auger-electron spectra.

For determining the ionic rest-frame energies, a nonrelativistic kinematic transformation relationship can be written in terms of the laboratory

electron energy E_L and emission angle θ_L , the ionic rest-frame energy E_A , the reduced beam energy (beam energy times the electron-carbon mass ratio) E_B , and the angle of the cone into which the beam scatters, θ_K ¹⁶⁻¹⁸:

$$E_A = E_L + E_B - 2(E_L E_B)^{1/2} \cos \theta_L \cos \theta_K. \quad (1)$$

In order to establish the absolute energy scale (E_A) in the center-of-mass system, the velocity of the emerging beam and the angle of electron ejection θ_L must be known. The incident beam energy was determined to within 0.3% by careful calibration of the analyzing magnet; but difficulties in determining beam direction and aligning the spectrometer made the physical determination θ_L uncertain. Additional systematic errors may contribute to the absolute ionic rest-frame energies. A major contribution is assumed to stem from uncertainties in the foil thickness. Together with the uncertainty in the incident beam energy and an uncertainty concerning the effective acceptance angle, which is assumed to be about 10%, an uncertainty of ± 1 eV in the experimental absolute energies of the individual peaks is estimated. To avoid the difficulties of the determination of E_B and θ_L , theoretical line energies for the $(1s2s^2)^2S - (1s^2\epsilon s)^2S$ and $(1s2s2p)^4P_{5/2}^o - (1s^2\epsilon f)^2F_{5/2}^o$ transitions were used as energy calibration points. The energies of these transitions were determined to be 227.5 eV for the $(1s2s^2)^2S$ and 229.9 eV for the $(1s2s2p)^4P^o$ state. In this connection it is important to note that photon observations in the CIV system are also available.^{4,19} Thus, a few term energies relative to the $(1s2s2p)^4P^o$ state are known with high accuracy. Using Eq. (1) and assuming negligible energy loss in the foil, the mean laboratory emission angle θ_L is thus determined to be 23.7° . Then, the energies of the resolved and identified line structures relative to the lowest-lying peaks in the prompt and delayed emission spectra [$(1s2s^2)^2S$ and $(1s2s2p)^4P^o$, respectively] are given within ± 0.3 eV accuracy.

Because of the finite acceptance angle of the spectrometer, Auger electrons are detected for a finite range of emission angles θ_L . The range of θ_L accepted by the spectrometer is further increased by the finite angular spread and scattering of the beam. The finite range of θ_L results in broadening of measured lines. An expression for the broadening caused by the effect of the finite acceptance angles can be obtained by differentiation of Eq. (1) with respect to θ_L ¹³

$$\Delta B_{\theta_L} = \Delta \theta_L 2(E_L E_B)^{1/2} \sin \theta_L \cos \theta_K. \quad (2)$$

An approximate relation for the maximum contribution to the measured linewidth from kinematic broadening caused by scattering of the beam has

been given by Rudd and Macek¹⁶ as

$$\Delta B_K = 4(E_L E_B)^{1/2} \sin\theta_L \sin\theta_K. \quad (3)$$

For the collisions studied in this experiment, these two contributions to line broadening are expected to be dominant. From Eqs. (2) and (3) values of 0.2% and 0.3%, respectively, have been estimated. Other line-broadening effects caused by the variation of θ_K within an interval $\Delta\theta_K$ ¹⁸ and the Berry effect³⁴ are considered to be negligible for MeV-range collision energies. We further note that the spectroscopic resolution for the carbon Auger-electron spectra was determined to be 0.6% (FWHM), which is large compared to the instrumental resolution. More detailed discussions of Auger-electron line broadening are given in articles by Rudd and Macek,¹⁶ and Stolterfoht *et al.*¹⁸

III. TERM ENERGIES

In order to make assignments of the experimental spectra we performed *ab initio* calculations on ten carbon 1s-hole states. For this purpose we used the generalized-Brillouin-theorem (GBT) multiconfiguration (MC) method of Schwarz and Chang,²⁰ which in practice will yield upper bounds to the energies of core-excited states. The details are given elsewhere.²⁰ In brief, the wave function of the system under study was approximated by

$$\Psi = \sum_{\nu} C_{\nu} \Psi_{\nu}(\varphi_i), \quad (4)$$

where (φ_i) is a set of atomic orbitals, the Ψ_{ν} are

LS configurations formed from these orbitals, and the C_{ν} are linear variational coefficients. The C_{ν} and Ψ_i were simultaneously optimized, until the M th root of the secular problem corresponding to Eq. (4) had reached its minimum under the constraint that Ψ is noninteracting with all singly de-excited states. Therefore only a few lower configurations had actually to be included in expansion (4) in order to obtain a variationally stable excited-state wave function (see Ref. 20).

The correlation in the valence shell was estimated within the framework of Sinanoğlu's many-electron theory.²¹ The internal and the most important semi-internal configurations were included in the MC expansion (4) as listed in Table I. The calculated MC energies are given in column 6 of Table I. These values were corrected for the estimated basis set defect,²⁰ the relativistic energy contribution, and the reduced-mass effect. The corrected energy values are listed in column 7 of Table I. To these energies we then added Sinanoğlu's all-external pair correlation energy increments²¹ of the core and valence shells, as given in column 8 of Table I. In addition, the final energies of the carbon hole states (column 9) were subtracted from the experimental energies of the ground states of the corresponding ions.²² The hole-state excitation energies thus obtained (column 10) are expected to be accurate within a few 0.1 eV. In this connection it should be emphasized that Nicolaides²³ has given an energy of 306.7 eV for the $(1s2p^2)^3D$ resonance in C IV, which is in close agreement with our MC energy.

In Tables II and III experimental line energies,

TABLE I. Calculated energy values of some prominent core-excited states in carbon (energies are given in eV).

Ion	State	Leading configuration ^a	Additional configurations ^a	Total number of configs.	Calc. energy	Corrected energy ^b	External correl.		Excitation energy ^c
							Energy	Energy	
1	2	3	4	5	6	7	8	9	10
C ⁰	¹ S ^o	1s2s2p ³ 3s		1	-734.9 ₁	-735.1 ₅	1.2	-736.3 ₅	293.7
C ⁺	⁶ S ^o	1s2s2p ³		1	-731.0 ₇	-731.3	1.1	-732.4	286.4
C ²⁺	³ P	1s2s2p ²		1	-700.2 ₈	-700.5	0.6	-701.1	293.3
	³ P ^o	1s2s ² 2p	1s ² 2s2p, 1s2s2p3d(3), 1s2p ³	6	-701.8 ₁	-702.0 ₅	0.5 ₅	-702.6	291.8
C ³⁺	¹ P ^o	1s2s ² 2p	1s ² 2s2p, 1s2s2p3d(2), 1s2p ³	5	-699.1 ₆	-699.4	0.6	-700.0	294.4
	² S ^e	1s2s ²	1s ² 2s, 1s2p ²	3	-654.0 ₆	-654.3	0.2 ₅	-654.5 ₅	292.0
	² P ^o ^d	1s2s2p(2)	1s ² 2p, 1s2p3d(2)	5	-645.6 ₈	-645.8	0.3	-646.1	300.4
	² P ^o ^e	1s2s2p(2)	1s ² 2p, 1s2p3d(2)	5	-641.9 ₀	-642.1 ₅	0.5 ₅	-642.7	303.8
	² D	1s2p ²	1s ² 3d, 1s2s3d(2)	4	-638.7 ₆	-639.0	0.7	-639.7	306.8
	² S	1s2p ²	1s ² 2s, 1s2s ²	3	-631.5 ₂	-631.7 ₅	1.3	-633.0 ₅	313.5

^a The number in parentheses behind a configuration refers to the number of different spin couplings.

^b Corrected for estimated basis set defect, relativistic contributions and for reduced-mass effect.

^c Excitation energies as measured from the corresponding ground state.

^d $^2P^o = 1s(2s2p^3P^o)^2P^o$.

^e $^2P^o = 1s(2s2p^1P^o)^2P^o$.

TABLE II. Electron energies (eV, ionic rest frame) for Coulomb autoionizing transitions involving initial configurations with two, three, and four electrons in highly ionized carbon. The predicted transition energies are given from various approximation methods.

Peak number	Peak energy	Initial state	Final ionic state	Predicted transition energy (eV)
1	227.5	$(1s2s^2)^2S$	$1s^2$	227.5 ^a
2	235.5	$(1s2s^22p)^3P^o$	$1s^22p$	235.9 ^a
		$1s(2s2p^3P^o)^2P^o$	$1s^2$	235.9 ^a
3	239	$(1s2s^22p)^1P^o$	$1s^22p$	238.5 ^a
		$1s(2s2p^1P^o)^2P^o$	$1s^2$	239.3 ^a
4	242	$(1s2p^2)^1D$	$1s^2$	242.3 ^a
5	243	$(1s2s^22p)^3P^o$	$1s^22s$	243.9 ^a
		$1s(2s2p^2^4P)^3P$	$1s^22p$	243.6 ^b
		$(1s2s2p^2)^3D$	$1s^22p$	244.3 ^b
6	246.5	$(1s2s^22p)^1P^o$	$1s^22s$	246.5 ^a
7	249	$(1s2s2p^2)^3S$	$1s^22p$	248.2 ^b
		$(1s2s2p^2)^1D$	$1s^22p$	248.3 ^b
		$(1s2p^2)^2S$	$1s^2$	249.0 ^a
		$1s(2s2p^2^2P)^3P$	$1s^22p$	249.9 ^b
8	253	$(1s2s2p^2)^1S$	$1s^22p$	252.2 ^b
		$(1s2s2p^2)^3D^o$	$1s^22s$	252.3 ^b
		$(1s2p^3)^3D$	$1s^22p$	253.7 ^b
9	255.5	$(1s2p^3)^1D^o$	$1s^22p$	255.6 ^b
		$(1s2s2p^2)^3S$	$1s^22s$	256.2 ^b
		$(1s2s2p^2)^1D$	$1s^22s$	256.3 ^b
10	258.5	$(1s2p^3)^3P^o$	$1s^22p$	257.4 ^b
		$(1s2p^3)^1P^o$	$1s^22p$	259.4 ^b
		$(1s2s2p^2)^1S$	$1s^22s$	260.2 ^b
11	265.5	$(2s^2)^1S$	$1s$	264.6 ^c
		$(2s2p)^3P^o$	$1s$	266.0 ^c
12	271	$(1s2s^3S)3s^2S$	$1s^2$	269.6 ^h
		$(1s2s^3S)3p^2P^o$	$1s^2$	272.2 ^c
13	274	$(2s^22p)^2P^o$	$(1s2p)^1P^o$	273.1 ^g
		$(2p^2)^1D$	$1s$	273.1 ^e
		$(1s2s^3S)3d^2D$	$1s^2$	273.9 ^h
		$(2s2p)^1P^o$	$1s$	274.0 ^c
		$(2s^22p)^2P^o$	$(1s2p)^3P^o$	276.7 ^g
		$(2s^22p)^2P^o$	$(1s2s)^1S$	276.7 ^g
14	278	$(1s2s^1S)3l$	$1s^2$	≈280 ^d
		$(1s2p^3P)3l$	$1s^2$	≈281 ^d
15	284	$(2s^22p)^2P^o$	$(1s2s)^3S$	282.1 ^g
		$(1s2p^1P)3l$	$1s^2$	≈284 ^d
16	286	$(2s2p^2)^2S$	$(1s2p)^1P^o$	285.2 ^g
		$(1s2s^3S)4l$	$1s^2$	≈286 ^d
17	290	$(2s2p^2)^2S$	$(1s2p)^3P^o$	288.7 ^g
		$(2s2p^2)^2S$	$(1s2s)^1S$	288.7 ^g
		$(1s2s^1S)4l$	$1s^2$	≈291 ^d
		$(1s2p^3P)4l$	$1s^2$	≈291 ^d
18	293	$(2s2p^2)^2S$	$(1s2p)^3P^o$	294.2 ^g
		$(1s2p^1P)4l$	$1s^2$	≈295 ^d
19	299			
	Series limit	$(1s2s)^3S\infty l$	$1s^2$	298.96 ^f
20	304	$(1s2s)^1S\infty l$	$1s^2$	304.39 ^f
	Series limit	$(1s2p)^3P^o\infty l$	$1s^2$	304.42 ^f
21	308			
	Series limit	$(1s2p)^1P\infty l$	$1s^2$	307.95 ^f
22	329	$2l3l$	$1s$	≈329.7 ^d
23	346	$2l4l$	$1s$	≈346.2 ^d

^aThis work (MCM method).^bSafronova *et al.* (Ref. 24).^cPerrot *et al.* (Ref. 26).^dThis work (quantum defect model).^eFeldman *et al.* (Ref. 27).^fBashkin and Stoner (Ref. 28).^gAhmed and Lipsky (Ref. 29).^hBerry (Ref. 4).

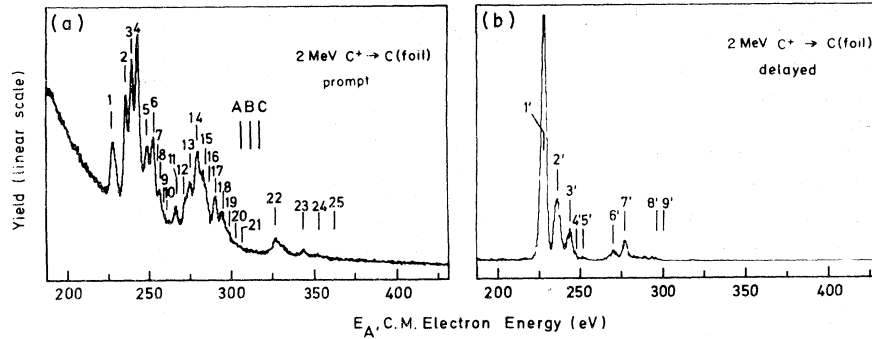


FIG. 1. Electron decay-in-flight spectra from auto-ionizing states of 2-MeV highly stripped carbon ions plotted in the rest frame of the emitting ion. The left spectrum (a) refers to a "foil-zero" position; the right spectrum (b) to a time delay of about 2.0 nsec.

as deduced from this study, are tabulated along with theoretical transition energies of multiply and core-excited states of two- to four-electron carbon ions. Referring to Table II, we see that the theoretical predictions are in good agreement with experiment. The predicted energies which are indicated by label "a," were deduced from Table I. Additional transition energies were determined from the work of Safronova *et al.*²⁴ (indicated by label "b" in Table II and III). Furthermore, we estimated transition energies (indicated by label "c" in Table III) for some quartet states in C IV. These values stem from the data of HolØien and Geltman,²⁵ who have applied the conventional Rayleigh-Ritz variational method to obtain the eigenvalues of the five lowest-lying states with symmetries $^4P^o$, 4P , 4S for three-electron atomic systems. We note that the $(1s2p^2)^4P = ^4P(1)$, $(1s2s3s)^4S = ^4S(1)$, and $(1s2s4s)^4S$

$= ^4S(2)$ energies [relative to the $(1s2s2p)^4P^o = ^4P^o(1)$ level of HolØien and Geltman] are in good agreement with those of Berry *et al.*^{4,19} In addition, various energy levels of the $1s2lnl'$ ($n \geq 3$) states in C IV and the $2lnl'$ ($n \geq 3$) states in C V were estimated using the simple quantum defect model (indicated by label "d" in Table II). We further comment that the calculated transition energies as listed in Table II and III have absolute and relative uncertainties smaller than the experimental errors. In summary, the extracted autoionization energies appear to be in good accord with the calculated transition energies. A detailed discussion of the spectra and the line identification is given in the following.

IV. RESULTS AND DISCUSSION

In Fig. 1(a) and 1(b) high-resolution beam-foil Auger-electron spectra are displayed. The prompt

TABLE III. Electron energies (eV, ionic rest frame) for metastable autoionizing transitions involving initial core-excited two- to four-electron carbon ions. The predicted transition energies are obtained using different approximation methods.

Peak number	Peak energy (eV)	Spectroscopic assignment (Initial state)	Final ionic state	Predicted transition energy (eV)
1'	229.9	$(1s2s2p)^4P^o^\dagger$	$1s^2$	229.9 ^c
2'	238	$(1s2s2p^2)^5P$ $(1s2p^2)^4P^\dagger$	$1s^22p$ $1s^2$	237.5 ^a 239.1 ^c
3'	245	$(1s2s2p^2)^5P$	$1s^22s$	245.5 ^a
4'	250	$(1s2p^3)^5S^o$ (?)	$1s^22p$	250.5 ^b
5'	255	$(1s2p^3)^3S^o$ (?)	$1s^22p$	254.4 ^b
6'	270	$(1s2s3s)^4S^\dagger$ $(1s2s3p)^4P^o^\dagger$	$1s^2$ $1s^2$	269.3 ^c 272.2 ^c
7'	279	$(1s2s4p)^4P^o^\dagger$ $(1s2s4s)^4S^\dagger$	$1s^2$ $1s^2$	276.5 ^c 278.6 ^c
8'	299	Series limit $(1s2s)^3S \infty l$	$1s^2$	298.96 ^d
9'	304	Series limit $(1s2p)^3P^o \infty l$	$1s^2$	304.42 ^d

^aThis work (MC method).

^bSafronova *et al.* (Ref. 24).

^cHolØien and Geltman (Ref. 25).

^dBashkin and Stoner (Ref. 28).

[†] $(1s2s2p)^4P^o = ^4P^o(1)$; $(1s2p^2)^4P = ^4P(1)$; $(1s2s3s)^4S = ^4S(1)$; $(1s2s3p)^4P^o = ^4P^o(2)$; $(1s2s4p)^4P^o = ^4P^o(3)$; $(1s2s4s)^4S = ^4S(2)$.

spectrum [Fig. 1(a)] refers to a "foil-zero" position, the delayed spectrum [Fig. 1(b)] to a time delay of about 2 nsec, respectively. From these spectra, experimental line energies were deduced by fitting the resolved and identifiable lines with a series of Gaussian functions. The prompt Auger spectrum is superimposed on a continuous background of electrons resulting from direct collision processes. This background was determined by fitting a second-order polynomial to the logarithm of the continuum on each side of the Auger groups. The line fit for the prompt spectrum was carried out after subtraction of the continuous background. The beam energy of about 2 MeV was chosen to optimize the production of Li-like carbon states. Therefore, the carbon projectiles emerging from the foil are primarily C^{3+} with significant C^{4+} and C^{2+} ions present as well.

The observed autoionization peaks are arbitrarily numbered in order of increasing energies. A general feature of the prompt and delayed spectra in Figs. 1(a) and 1(b) is the concentration of peaks into three and two basic groups, respectively. It is assumed that in the prompt spectrum the energetically lowest lying and most intense peak group can be attributed mainly to initially core-excited three-electron systems. A comparison with theoretically predicted term energies indicates that the lines in the group are dominated by $1s2l'2l'$ configurations in CIV such as $1s2s^2$, $1s2s2p$, and $1s2p^2$. It is also seen from Fig. 1(a) that the CIV $(1s2p^2)^2D$ terms (peak 4) are strongly populated in 2-MeV $C^+ \rightarrow C$ -foil collisions. The line identification of the peaks labeled 5 and 6 is based on estimated energies for the initial $1s2s^22p^1$ and $1s2s2p^2$ configurations in CIII. We note that core-excited four-electron states can decay to the $1s^22s\epsilon l$ and the $1s^22p\epsilon l$ continua, giving rise to double peaks with an energy separation of about 8 eV. As an example, Fig. 2 displays the decay scheme of the $(1s2s^22p)^3P^0$ state in CIII. It is to be seen that the four-electron $(1s2s^22p)^3P^0$ states decay to the $1s^22s$ and the $1s^22p$ final ionic states. Thus, peak 5 is evidently an admixture of transitions as originating from the initial $(1s2s^22p)^3P^0$, $1s(2s2p^2^4P)^3P$, and $(1s2s2p^2)^3D$ levels in CIII. The peak labeled 6 in Fig. 1(a) can be assigned to the CIII $(1s2s^22p)^1P^0 \rightarrow (1s^22s\epsilon p)^1P^0$ transition. In addition, peaks 7-10 are ascribed on energetic grounds to Auger decays of core-excited four-electron systems. In the next-higher-energy group three-electron states arise from configurations which contain at least one electron in the $n=3$ shell or higher. A comparison to theoretically predicted energies indicates an overlap with doubly excited $2l'2l'$ states in CV and triply excited $2l'2l'nl''$ states²⁹ in CIV characterized by an empty, doubly

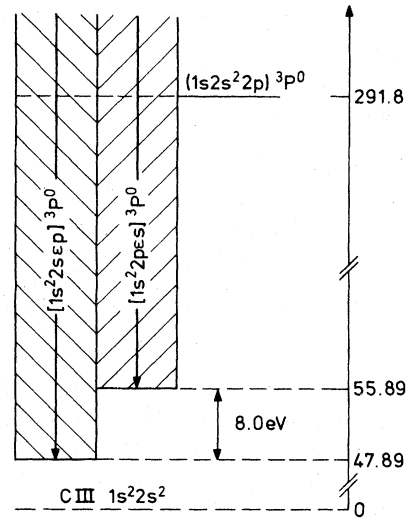


FIG. 2. Decay scheme for the $(1s2s^22p)^3P^0$ state in CIII. Energies are in eV.

ionized core (Table II). The lowest lying triply excited level is $(2s^22p)^2P^0$. Figure 3 illustrates the resulting decay scheme for this level. It is apparent from Fig. 3 that triply excited states are adjacent to the $(1s2s)^3^1S\epsilon l$ and the $(1s2p)^3^1P\epsilon l$ continua. Thus, the $(2s^22p)^2P^0$ states in CIV can undergo transitions to the $[1s2s(^3S)\epsilon p]^2P^0$, $[1s2s(^1S)\epsilon p]^2P^0$, $[1s2p(^3P^0)\epsilon s]^2P^0$, and $[1s2p(^1P^0)\epsilon s]^2P^0$ continua, where the $1s2s(^1S)$ and the $1s2p(^3P^0)$ thresholds are nearly degenerated in energy (see Fig. 3). Furthermore, lower-intensity three-electron autoionization transitions³⁰ such as $(2s^22p)^2P^0 \rightarrow (1s^2\epsilon p)^2P^0$, though less probable, are allowed as well.

Peak 11 may be assigned due to autoionization of $(2s^2)^1S$ and $(2s2p)^3P^0$ states in CV. The shoulder on the low-energy side of peak 13 (peak 12) is expected to occur from decays of the $(1s2s^3S)3s^2S$ and $(1s2s^3S)3p^2P^0$ states in CIV. In addition, peak

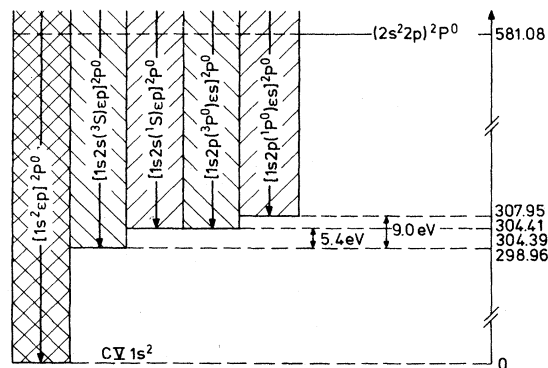


FIG. 3. Decay scheme for the $(2s^22p)^2P^0$ state in CIV. Energies are in eV.

13 should be composed of autoionization lines arising from the C IV $(2s^2 2p)^2 P^o$, CV $(2p^3)^1 D$, CIV $(1s2s^3 S)3d^2 D$, and CV $(2s2p)^1 P^o$ states, respectively. Peak 14 at about 278 eV should not be assigned to a single decay, since several transitions from closely spaced $(1s2s^1 S)3l$ and $(1s2p^3 P^o)3l$ levels in CIV are overlapping in this region. Similarly, the peak 15 on the high-energy side of peak 14 near 284 eV could be a cumulative effect of autoionizing CIV $(2s2p^2)^2 S$ and CIV $(1s2p^1 P^o)3l$ levels. Moreover, various autoionizing $1s2lnl'$ ($n \geq 4$) and $2l2l'nl''$ ($n \geq 2$) levels may be responsible for the structures 16–18.

The three lowest series limits for three-electron systems are indicated at the labels 19, 20, and 21. Above these limits lines resulting from the autoionizing decay of three-electron systems are very unlikely.

Figure 1(a) also shows two characteristic series limits of four-electron states, namely $(1s2s^2)^2 S^\infty l \rightarrow 1s^2 2s\epsilon l$ (indicated by label A) at about 292 eV and $(1s2p^2)^2 S^\infty l \rightarrow 1s^2 2p\epsilon l'$ (indicated by label B) at about 305.5 eV. We suggest that above 315.5 eV corresponding to the series limit $(1s2p^2)^2 S^\infty l \rightarrow 1s^2 2s\epsilon l'$ in C III (indicated by label C) contributions from four-electron systems are negligible. We further note that four-electron systems of the type $1s2l2l'nl''$ characterized by a three-electron core and a loosely attached nl'' electron, decay mainly via a "spectator" channel with the orbit of the outermost electron remaining unchanged. This leads to transition energies which are energetically lower lying than the series limits A, B, and C. Hence, the energetically higher-lying structures may be attributed to doubly excited He-like resonances in CV.

The highest energy group of peaks in the prompt spectrum is assumed to arise from $2lnl'$ configurations with a doubly ionized K shell and with one electron being excited into the $n = 3$ shell or higher. It is to be seen from Table II that the estimated $2l3l'$ and $2l4l'$ term energies are in good agreement with experiment, which is due to the fact that higher orbitals are involved and consequently screening and correlation effects are less effective.

The resolved spectral features in the prompt electron emission spectrum could be identified by comparison to theoretical line energies; Table II shows an absolute agreement within ± 1 eV. Line broadening due to the finite acceptance angular spread of the spectrometer and energy straggling, however, make a total identification of the foil excited prompt spectrum impossible. It is expected that many more lines remained unresolved owing to the great number of possible transitions.

Throughout the remainder of this section we

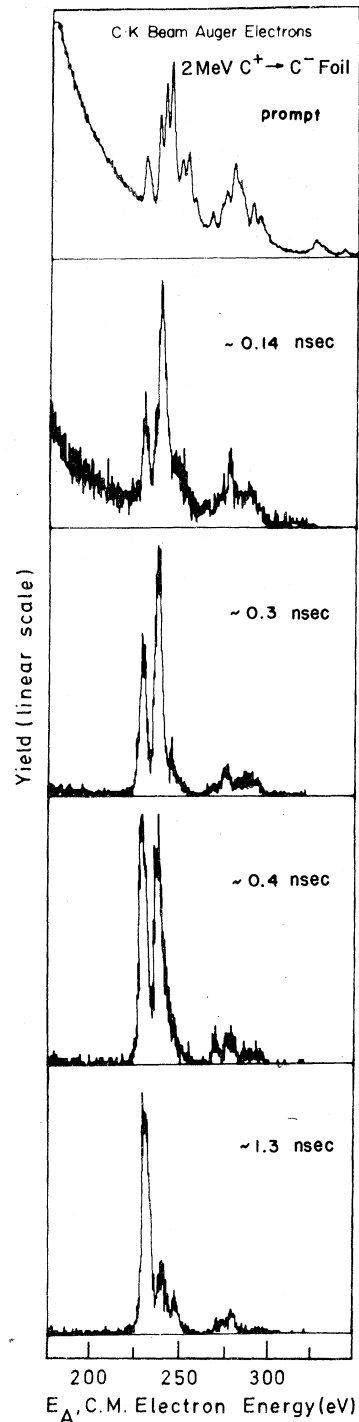


FIG. 4. Comparison of a "prompt" electron spectrum with different "delayed" spectra taken with the foil being moved to different upstream positions. The delay times are approximate because of uncertainties in the different foil positions.

discuss the spectral features in the delayed electron emission spectra as indicated in Figs. 1(b) and 4. Figure 1(b) represents a delayed spectrum recorded at a time delay of about ~ 2 nsec, corresponding to an upstream foil position of about 11 cm, and Fig. 4 compares various spectra taken for delay times between 0 and ~ 1.3 nsec. The prominent peaks in the delayed spectra [labeled 1' through 9' in Fig. 1(b)] are attributed to transitions from metastable autoionizing quartet states in CIV and quintet states in CIII. As can be seen from Fig. 4, the prompt decaying (Coulomb autoionizing) states which clearly dominate in the zero-delay spectrum are rapidly diminished when the foil is moved out of the focus of the electron analyzer. The lowest energy peak in the delayed spectra labelled 1' [see Fig. 1(b)] is attributed to the lithium-like $(1s2s2p)^4P^o$ state in CIV. This quartet state is metastable against both Coulomb autoionization and electric dipole (E1) transitions, whereas the energetically higher-lying quartet states such as $(1s2p^3P^o np)^4P$, $(1s2s^3Sn s)^4S$, $(1s2s^3Sn d)^4D$, and $(1s2p^3P^o nd)^4D^o$ are depleted mainly by allowed radiative decays to lower-lying quartet states.^{4,19} Because of the differential metastability within the fine-structure levels ($J = \frac{1}{2}, \frac{3}{2}, \frac{5}{2}$) of the $(1s2s2p)^4P^o$ state, peak 1' is composed of three components having different lifetimes.

In the energy region near 238 eV (peak 2') decays from quartet states overlap with autoionization transitions arising from quintet states. More specifically, peak 2' originates from autoionizing transitions of the $(1s2p^2)^4P$ terms in CIV and $(1s2s2p^2)^5P$ terms in CIII. In this connection we note that the CIV $(1s2p^2)^4P$ states are preferentially depleted via optical decays to the $(1s2s2p)^4P^o$ states leading to a lifetime of 1.1 nsec.³¹ This may explain the decreasing intensity of peak 2' for increasing delay times. On the other hand the $(1s2s2p)^5P$ terms in CIII are both metastable with respect to Coulomb autoionization and electric dipole transitions. Therefore, at the largest delay time of about 2 nsec, peak 2' should be dominated by autoionizing transitions as originating from initial $(1s2s2p^2)^5P$ states. The peak labeled 3' in Fig. 1 can be clearly identified as resulting from the initial Be-like $(1s2s2p^2)^5P$ state by comparison to the theoretically predicted transition energy. The correct interpretation of this peak is also supported by the energy separation of ~ 7.5 eV between peak 3' and 2' which is close to the $1s^22s-1s^22p$ separation in CIV (see Fig. 3). For the higher-lying metastable four-electron states it is assumed that they decay mainly via optical transitions. Nevertheless, very weak lines labeled 4' and 5' are observed, which may be attributed to

initial Be-like $(1s2p^3)^5S^o$ and $(1s2p^3)^3S^o$ states in CIII.

The line structure around 275-eV center-of-mass electron energy could be identified as resulting from initial three-electron quartet states with one electron being excited into the $n=3$ or 4 shell. Another metastable autoionizing state would be $(1s2p^2)^2P$. However, no autoionizing decays associated with the CIV $(1s2p^2)^2P$ state were observed in the delayed spectrum. This might be due to the fact that the $(1s2p^2)^2P$ state decays preferentially by electrical dipole transitions with a short lifetime of about $\tau \leq 10^{-11}$ sec. Finally, no lines which could be attributed to metastable autoionizing sextet states [e.g., $(1s2s2p^3)^6S$] were found at 2 MeV beam energy. This is consistent with the result of a mean charge close to +3 for a 2-MeV carbon beam after penetrating a carbon foil.³²

V. CONCLUSION

In summary autoionization lines of two-, three-, and four-electron carbon ions have been identified from comparison between measured prompt and time-delayed electron decay-in-flight spectra and between calculated transition energies. The principal feature of this publication is the observation and identification of a large number of previously unidentified Coulomb and metastable autoionizing states. The deduced energy values and spectroscopic identifications might be useful for further discussions of theoretical approximations of wave functions for core-excited two- to four-electron states.

It is further anticipated that many more lines due to the great number of possible autoionization transitions remained unresolved. For an unambiguous interpretation of the closely spaced structures at higher energies the resolution of the apparatus must be improved. In addition, more advanced experimental techniques, such as electron-ion, electron-electron, and electron-photon coincidence measurements could help to classify presently unidentified lines.

ACKNOWLEDGMENTS

We are very much indebted to Dr. N. Stolterfoht and Dr. F. Hopkins for helpful and critical comments on the manuscript. Furthermore we are grateful to the Deutsche Forschungsgemeinschaft and to the Fonds der chemischen Industrie for financial support and to the Computational Center of the University of Bonn for computer time.

- ¹D. L. Matthews, B. M. Johnson, J. J. Mackey, and C. F. Moore, *Phys. Rev. Lett.* **31**, 1331 (1973).
- ²D. Schneider, C. F. Moore, and B. M. Johnson, *J. Phys.* **B 9**, L153 (1976); D. L. Matthews, R. Fortner, D. Schneider, and C. F. Moore, *Phys. Rev. A* **14**, 1561 (1976).
- ³I. Martinson and A. Gaupp, *Phys. Rep.* **15C**, 113 (1974).
- ⁴H. G. Berry, *Phys. Scr.* **12**, 5 (1975).
- ⁵B. Donnally, W. W. Smith, D. J. Pegg, M. Brown, and I. A. Sellin, *Phys. Rev. A* **4**, 122 (1971).
- ⁶I. A. Sellin, D. J. Pegg, M. Brown, W. W. Smith, and B. Donnally, *Phys. Rev. Lett.* **27**, 1108 (1971).
- ⁷I. A. Sellin, D. J. Pegg, P. M. Griffin, and W. W. Smith, *Phys. Rev. Lett.* **28**, 1229 (1972).
- ⁸D. J. Pegg, I. A. Sellin, P. M. Griffin, and W. W. Smith, *Phys. Rev. Lett.* **28**, 1615 (1972).
- ⁹H. H. Haselton, R. S. Thoe, J. R. Mowat, P. M. Griffin, D. J. Pegg, and I. A. Sellin, *Phys. Rev. A* **11**, 468 (1975).
- ¹⁰B. R. Junker and J. W. Bardsley, *Phys. Rev. A* **8**, 1345 (1973).
- ¹¹D. J. Pegg, I. A. Sellin, R. Peterson, J. R. Mowat, W. W. Smith, M. D. Brown, and J. R. MacDonald, *Phys. Rev. A* **8**, 1350 (1973).
- ¹²I. A. Sellin, *Nucl. Instr. Meth.* **110**, 477 (1973).
- ¹³B. M. Johnson, D. Schneider, W. Hodge, K. S. Robert, Y. Whinton, and C. E. Moore, (unpublished).
- ¹⁴B. M. Johnson, D. Schneider, K. S. Roberts, J. E. Bolger, and C. F. Moore, *Phys. Lett.* **53A**, 254 (1975).
- ¹⁵D. Schneider, W. Hodge, B. M. Johnson, L. E. Smith, and C. F. Moore, *Phys. Lett.* **54A**, 174 (1975).
- ¹⁶M. E. Rudd and J. Macek, in *Case Studies in Atomic Physics*, edited by W. E. McDaniels and M. C. McDowell (North-Holland, Amsterdam, 1973), Vol. 3, p. 47.
- ¹⁷D. J. Pegg, I. A. Sellin, R. Peterson, J. R. Mowat, W. W. Smith, M. D. Brown, and J. R. MacDonald, *Phys. Rev. A* **8**, 1350 (1973).
- ¹⁸N. Stolterfoht, D. Schneider, D. Burch, B. Aagaard, E. Bøving, and B. Fastrup, *Phys. Rev. A* **12**, 1313 (1975).
- ¹⁹H. G. Berry, M. C. Buchet-Poulizac, and J. P. Buchet, *J. Opt. Soc. Am.* **63**, 240 (1973).
- ²⁰W. H. E. Schwarz and T. C. Chang, *Int. J. Quantum Chem.* **10S**, 91 (1975); T. C. Chang and W. H. E. Schwarz, *Theor. Chim. Acta* (to be published).
- ²¹O. Sinanoğlu, *At. Phys.* **2**, 131 (1969).
- ²²C. E. Moore, *Atomic Energy Levels*, NBS Circ. 467 (U.S. GPO, Washington, D.C., 1948).
- ²³C. A. Nicolaidis, *Nucl. Instr. Meth.* **110**, 231 (1973).
- ²⁴U. I. Safronova and V. N. Kharitonova, *Opt. Spektrosk.* **27**, 550 (1969) [*Opt. Spectrosc.* **27**, 300 (1969)].
- ²⁵E. Holbøien and S. Geltman, *Phys. Rev.* **153**, 81 (1967).
- ²⁶R. H. Perrot and A. L. Stewart, *J. Phys. B* **1**, 381 (1968); Y. M. C. Chan and A. L. Stewart, *Proc. Phys. Soc.* **90**, 619 (1967).
- ²⁷U. Feldman and L. Cohen, *Astrophys. J.* **158**, L169 (1969).
- ²⁸S. Bashkin and J. O. Stoner, *Atomic Energy Levels and Grotrian Diagrams* (North-Holland, Amsterdam, 1975).
- ²⁹M. Ahmed and L. Lipsky, *Phys. Rev. A* **12**, 1176 (1975).
- ³⁰R. Bruch, G. Paul, J. Andrä, and L. Lipsky, *Phys. Rev. A* **12**, 1808 (1975).
- ³¹I. Martinson, *Nucl. Instr. Meth.* **90**, 81 (1971).
- ³²J. B. Marion and F. C. Young, *Nuclear Reaction Analysis* (North-Holland, Amsterdam, 1968).
- ³³D. L. Matthews, B. M. Johnson, J. J. Mackey, L. E. Smith, W. Hodge, and C. F. Moore, *Phys. Rev. A* **10**, 1177 (1974).
- ³⁴H. W. Berry, *Phys. Rev.* **121**, 1714 (1961); R. B. Barker and H. W. Berry, *Phys. Rev.* **151**, 141 (1966).